Acta Crystallographica Section F
Structural Biology and Crystallization Communications
ISSN 1744-3091

N-terminal truncation enables crystallization of the receptor-binding domain of the FedF bacterial adhesin

Maia De Kerpel,[a] Inge Van Molle,[a] Lea Brys,[b] Lode Wyns,[a] Henri De Greve[a] and Julie Bouckaert[a]*

[a]Department of Ultrastructure, Vrije Universiteit Brussel (VUB), Flanders Interuniversity Institute for Biotechnology (VIB), Pleinlaan 2, 1050 Brussels, Belgium, and [b]Department of Cellular and Molecular Immunology, Vrije Universiteit Brussel (VUB), Flanders Interuniversity Institute for Biotechnology (VIB), Pleinlaan 2, 1050 Brussels, Belgium

Correspondence e-mail: bouckaej@vub.ac.be

Received 28 September 2006
Accepted 17 November 2006

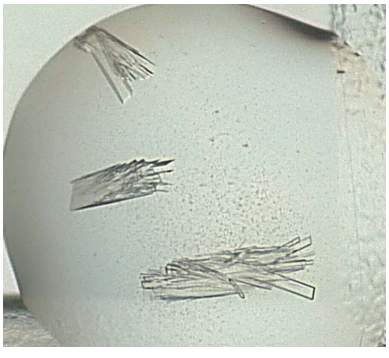

FedF is the two-domain tip adhesin of F18 fimbriae from enterotoxigenic *Escherichia coli*. Bacterial adherence, mediated by the N-terminal receptor-binding domain of FedF to carbohydrate receptors on intestinal microvilli, causes diarrhoea and oedema disease in newly weaned piglets and induces the secretion of Shiga toxins. A truncate containing only the receptor-binding domain of FedF was found to be further cleaved at its N-terminus. Reconstruction of this N-terminal truncate rendered FedF amenable to crystallization, resulting in crystals with space group $P2_12_12_1$ and unit-cell parameters a = 36.20, b = 74.64, c = 99.03 Å that diffracted to beyond 2 Å resolution. The binding specificity of FedF was screened for on a glycan array, exposing 264 glycoconjugates, to identify specific receptors for cocrystallization with FedF.

1. Introduction

Post-weaning diarrhoea and oedema disease in piglets are caused by pathogenic *Escherichia coli* strains, including enterotoxigenic *E. coli* (ETEC) and Shiga toxin-producing *E. coli* (STEC). These strains produce F18 fimbriae that mediate the adherence of the bacteria to the microvilli of the epithial surface cells in the duodenum (Bertschinger *et al.*, 1990; Gyles *et al.*, 1998) and also secrete toxins during the infection process. The Shiga toxin Stx_{2e} variant is secreted by F18ab-positive *E. coli* and reaches its target host cell *via* the bloodstream, resulting in the accumulation of fluid (oedema disease) and neurological disorders. F18ac-positive *E. coli* cause post-weaning diarrhoea by the expression of heat-stable enterotoxins (Kapitany *et al.*, 1979).

F18 fimbriae are expressed by the *fed* gene cluster, with *fedA* encoding the major subunit (Imberechts *et al.*, 1992), *fedB* the outer membrane usher, *fedC* the periplasmic chaperone and *fedE* and *fedF* minor pilus subunits. FedE and FedF are the F18 minor subunits essential for fimbrial adhesion and also regulate the length of the F18 fimbriae, which are normally 1–2 µm in length (Imberechts *et al.*, 1996). FedF was shown to be the F18 tip adhesin (Smeds *et al.*, 2001). Its pilin domain connects to the FedA polymer *via* multiple copies of FedE (Hahn *et al.*, 2000). Tip adhesins can typically be divided into two immunoglobulin-like domains: an N-terminal lectin or receptor-binding module and a C-terminal pilin. Like all major and minor pilins, the pilin domains of adhesins also lack the last β-strand G of their immunoglobulin fold (Ig-fold). Therefore, the adhesin is not a stable protein by itself, but needs to be donor-strand complemented (Choudhury *et al.*, 1999; Sauer *et al.*, 1999). The missing strand is donated by a specific chaperone in the periplasm and by the next pilin in the pilus.

In the absence of the chaperone, soluble self-complementing and swapped pilin dimers (Jędrzejczak *et al.*, 2006; Van Molle *et al.*, in preparation) and trimers (Pettigrew *et al.*, 2004; Korotkova *et al.*, 2006) are formed and their crystal structures have been reported. Here, the pilins use different methods to complement their Ig-fold other than using the N-terminal extension of the neighbouring pilin domain. Because of misfolding, the pilins in these oligomers are incompetent for assembly into fimbriae or pili. On the other hand, crystal structures of typical tip adhesins have been mostly determined

using genetic constructs that are truncated after the receptor-binding domain of the adhesin. Owing to the compact size of these domains (typically 15–18 kDa), their crystals usually diffract beyond 2 Å resolution. Examples are the fimbrial receptor-binding domains of PapG-II (Dodson *et al.*, 2001) and of FimH (Bouckaert *et al.*, 2005) from uropathogenic *E. coli* and of F17G from ETEC (Buts, Bouckaert *et al.*, 2003).

In the current study, we report the cloning, expression, purification and crystallization of the receptor-binding domain of the FedF adhesin present on F18 fimbriae. Of all the constructs of FedF produced in this research, only one form, $FedF_{15–165}$ (151 amino acids, 16.3 kDa), could be crystallized. Crystallization required not only C-terminal but also N-terminal truncation of the FedF adhesin. Screening delivered one succesful crystallization condition from almost 500 trials using the EMBL high-throughput crystallization facility. Microcrystals could be mounted directly from the screen and flash-frozen for high-resolution data collection at the DESY synchrotron in Hamburg, Germany.

2. Materials and methods

2.1. Cloning, expression and purification and characterization of FedF truncates

The *fedF* gene from the F18$^+$ *E. coli* 107/86 strain (Imberechts *et al.*, 1996; gene accession No. Z26520) was cloned in the pDEST14 vector under a T7 promotor (Gateway technology, Invitrogen). The gene was truncated after Ala110 and Lys165, respectively, in order to express only the receptor-binding domain of FedF (Fig. 1). This choice was based partly on secondary-structure predictions, to avoid truncation within a clearly defined secondary-structure element (Rost & Liu, 2003), and partly on amino-acid alignments with fimbrial pilin domains of known three-dimensional structure. The resulting truncates were transformed into *E. coli* strain C43 (DE3) (Miroux & Walker, 1996). The C43 (DE3) cells were grown in Luria–Bertani (LB) medium until the OD_{600} reached 0.5, induced with 1 m*M* IPTG and incubated for a further 2 h. Cells were subjected to osmotic shock and the periplasmic extract was loaded onto an Ni–NTA affinity column (Qiagen) in 1 *M* NaCl, 20 m*M* Tris pH 7.5 and 10 m*M* imidazole. Bound protein was eluted with the same buffer and 1 *M* imidazole. C-terminally His-tagged proteins were further purified using gel filtration on a Superdex-75HR column in 10 m*M* HEPES pH 7.0 and 150 m*M* NaCl.

Gene constructs encoding truncated FedF proteins without a His tag were expressed in the same way. The periplasmic extract was loaded onto a Source 30S column (Amersham) for cation exchange in 20 m*M* Tris pH 7.5 and eluted using an NaCl gradient at a concentration of 140 m*M* NaCl. Subsequently, the same gel-filtration procedure was used as for the His-tagged proteins.

The identity of purified $FedF_{1–165H6}$ was first confirmed using an anti-His Mab on a Western blot as described in Coligan *et al.* (2002). The nitrocellulose membrane was blocked overnight at 277 K with phosphate-buffered saline complemented with 1% casein. The membrane was incubated with the primary antibody at room temperature for 2 h. Goat anti-mouse or anti-rabbit antibodies conjugated with peroxidase were then added for 1 h. The membrane was developed using H_2O_2. The purified $FedF_{1–165H6}$ was injected in complete Freund adjuvant intradermally in a rabbit, with the purpose of obtaining a polyclonal rabbit anti-$FedF_{1–165H6}$ serum. After three weeks, a boost was given by injecting $FedF_{1–165H6}$ in incomplete Freund adjuvant. Serum containing rabbit anti-FedF was taken after another 10 d.

N-terminal sequencing (Alta Bioscience) was performed after electrotransfer of $FedF_{v1–165}$ from a 12.5% SDS–PAGE onto a

```
                                  1         .         .         .         .        50
FedF1-110H6      MRLKYILIIPLLLISLSVFA  STLQVDKSVSYDWINSSASSAQVTGTLLGTGKTNTTQMPALYTWQHQIYN
FedF1-165H6      MRLKYILIIPLLLISLSVFA  STLQVDKSVSYDWINSSASSAQVTGTLLGTGKTNTTQMPALYTWQHQIYN
FedF1-165        MRLKYILIIPLLLISLSVFA  STLQVDKSVSYDWINSSASSAQVTGTLLGTGKTNTTQMPALYTWQHQIYN
FedF1-160        MRLKYILIIPLLLISLSVFA  STLQVDKSVSYDWINSSASSAQVTGTLLGTGKTNTTQMPALYTWQHQIYN
FedF1-162        MRLKYILIIPLLLISLSVFA  STLQVDKSVSYDWINSSASSAQVTGTLLGTGKTNTTQMPALYTWQHQIYN
FedFv1-165       MRLKYILIIPLLLISLSVFA  STLQVDKSVSYDWINSSTSSAQITGTLLGTGKTNTTQMPALYTWQHQIYN
FedF15-165       MKKTLIALAIAASAASGMAHA              NSSASSAQVTGTLLGTGKTNTTQMPALYTWQHQIYN
FedF13-165       MKKTLIALAIAASAASGMAHA            WINSSASSAQVTGTLLGTGKTNTTQMPALYTWQHQIYN

                           .         .         .         .       100       .         .
FedF1-110H6      VNFIPSSSGTLTCQAGTILVWKNGRETQYALECRVSIHHSSGSINESQWGQQSQVGFGTAHHHHHH
FedF1-165H6      VNFIPSSSGTLTCQAGTILVWKNGRETQYALECRVSIHHSSGSINESQWGQQSQVGFGTACGNKKCRFTG
FedF1-165        VNFIPSSSGTLTCQAGTILVWKNGRETQYALECRVSIHHSSGSINESQWGQQSQVGFGTACGNKKCRFTG
FedF1-160        VNFIPSSSGTLTCQAGTILVWKNGRETQYALECRVSIHHSSGSINESQWGQQSQVGFGTACGNKKCRFTG
FedF1-162        VNFIPSSSGTLTCQAGTILVWKNGRETQYALECRVSIHHSSGSINESQWGQQSQVGFGTACGNKKCRFTG
FedFv1-165       VNFIPSSSGTLTCQAGTILVWRDGRETQYALECRVSIHHSSGSINESQWGQQSQVGFGTACGTKKCRFTG
FedF15-165       VNFIPSSSGTLTCQAGTILVWKNGRETQYALECRVSIHHSSGSINESQWGQQSQVGFGTACGNKKCRFTG
FedF13-165       VNFIPSSSGTLTCQAGTILVWKNGRETQYALECRVSIHHSSGSINESQWGQQSQVGFGTACGNKKCRFTG

                           .         .       150         .         .
FedF1-165H6      FEISLRIPPNAQTYPLSSGDLKGSFSLTNKEVNWSASIYVPAIAKHHHHHH
FedF1-165        FEISLRIPPNAQTYPLSSGDLKGSFSLTNKEVNWSASIYVPAIAK
FedF1-160        FEISLRIPPNAQTYPLSSGDLKGSFSLTNKEVNWSASIYV
FedF1-162        FEISLRIPPNAQTYPLSSGDLKGSFSLTNKEVNWSASIYVPA
FedFv1-165       FEISLRIPPNAQMYPLSSGDLKGSFSLTNKEVNWSASIYVPAIAK
FedF15-165       FEISLRIPPNAQTYPLSSGDLKGSFSLTNKEVNWSASIYVPAIAK
FedF13-165       FEISLRIPPNAQTYPLSSGDLKGSFSLTNKEVNWSASIYVPAIA
```

Figure 1
Amino-acid sequence alignment of the FedF truncates. The first residue of the mature protein, after cleavage of the signal peptide, is labelled 1. Differences from the $FedF_{v1–165}$ variant are indicated in bold. The two N-termini found for $FedF_{1–165}$ are underlined.

Table 1
Data-collection and processing for $FedF_{15–165}$.

Values in parentheses are for the highest resolution shell (2.07–2.00 Å).

Space group	$P2_12_12_1$
Unit-cell parameters (Å)	a = 36.20, b = 74.64, c = 99.03
Unit-cell volume (Å^3)	267578
Resolution range (Å)	42–2.0
Reflections (total/unique)	100446/18666
Completeness (%)	98.9 (98.8)
R_{merge}† (%)	7.5 (12.1)
$\langle I/\sigma(I)\rangle$	18.5 (12.4)
Matthews coefficient (Å^3 Da^{-1})	2.05
Solvent content (%)	40.1
FedF molecules per ASU	2

† $R_{merge} = \sum_{\mathbf{h}}\sum_l |I_{\mathbf{h}l} - \langle I_{\mathbf{h}}\rangle| / \sum_{\mathbf{h}}\sum_l \langle I_{\mathbf{h}}\rangle$, where I_l is the lth observation of reflection **h** and $\langle I_{\mathbf{h}}\rangle$ is the weighted average intensity for all observations l of reflection **h**.

ProBlot PVDF membrane (Applied Biosystems) and excision of the bands corresponding to the estimated molecular weight upon staining with Coomassie R350.

2.2. Crystallization and crystal analysis

Screening for crystallization conditions for $FedF_{15–165}$ took place at the high-throughput crystallization facility at the EMBL in Hamburg (Germany) after in-house screening with commercially available screens (Crystal Screens 1 and 2 from Hampton Research) remained unsuccessful. Using the robot, 300 nl droplets of protein solution (24 mg ml^{-1} in 20 m*M* HEPES pH 7.5 and 140 m*M* NaCl) were mixed with 300 nl precipitant solution. Five sets of 96 precipitant conditions from both commercial and academically developed screens were used: Index, Crystal Screens I and II, Natrix and MembFac (Hampton Research), the JCSG screen (Newman *et al.*, 2005) and Jena 1–4 (Jena Bioscience). Crystals of the $FedF_{15–165}$ truncate were only obtained using the JCSG screen with 0.17 *M* ammonium sulfate, 25.5%(*w*/*v*) PEG 4000 and 15%(*v*/*v*) glycerol. Larger crystals were obtained at home using the same conditions and microseeding.

Prior to data collection, a microcrystal of $FedF_{15–165}$ was directly mounted from the JCSG screen in a nylon cryoloop (Hampton Research) and placed directly into a nitrogen-gas stream at 100 K at beamline X12 of the EMBL Outstation Hamburg, Germany. The data were processed using *DENZO*, *XDISPLAYF* and *SCALEPACK* from the *HKL* package (Otwinowski & Minor, 1997) and *TRUNCATE* from the *CCP*4 suite (Collaborative Computational Project, Number 4, 1994). Crystal parameters and data-processing statistics are summarized in Table 1.

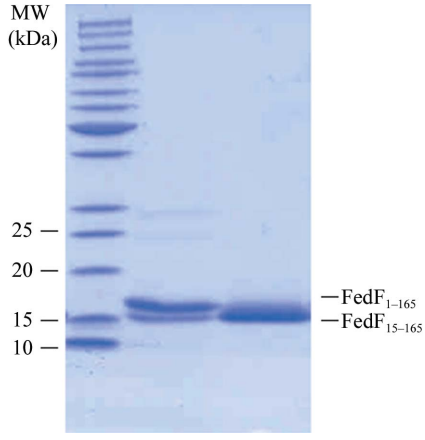

Figure 2
$FedF_{1–165}$ (lane 2) showing two bands on 12% SDS–PAGE, the N-terminal truncate $FedF_{15–165}$ (lane 3) and PageRuler protein ladder (Fermentas SM0661; lane 1).

2.3. Screening of carbohydrate binding of FedF on a glycan microarray

The carbohydrate-specificity of the $FedF_{1–165}$ receptor-binding domain of the FedF fimbrial adhesin from the F18$^+$ *E. coli* 107/86 strain was screened against printed array version 2. Slides (Schott Nexterion H slides, catalogue No. 1070936B) were printed at the Core D carbohydrate-synthesis/protein-expression consortium located at the Scripps Research Institute. The slides exposed 264 immobilized glycans spotted at a concentration of 100 µ*M* and in six replicates (Blixt *et al.*, 2004). Preprinted slides were soaked in deionized water for 5 min at room temperature and dried in a stream of nitrogen. $FedF_{1–165}$ was diluted to the assay concentration of 100 µg ml^{-1} in 20 m*M* Tris–HCl pH 7.4, 150 m*M* NaCl, 2 m*M* $CaCl_2$ and 2 m*M* $MgCl_2$, the wash buffer, in the presence of 0.05% Tween-20 and 1% BSA, and 50 µl was applied to the printed surface and covered with a cover slip. The slide was incubated, protected from light, in a humidified chamber for 1 h at room temperature. A first wash step used the wash buffer with 0.05% Tween-20 and wash buffer alone for 10 s each. For detection, 50 µl rabbit anti-FedF was applied at 10 µg ml^{-1} and the slide was subsequently incubated and washed as described above. Finally, 50 µl labelled goat anti-rabbit IgG-488 was applied, incubated and washed again in the same way. After another 10 s wash in deionized water, the slide was dried in a nitrogen stream. The binding image was read by a Perkin–Elmer Microscanarray XL4000 scanner. Image analysis was performed using *Imagene* v.6 image-analysis software. The raw data results files were uploaded to the Consortium for Functional Glycomics database and webpages (http://www.functionalglycomics.org).

3. Results and discussion

Of the two FedF proteins, $FedF_{1–110H6}$ and $FedF_{1–165-H6}$, that were C-terminal truncates followed by a six-histidine tag, only $FedF_{1–165H6}$ was soluble (Fig. 1). However, it did not crystallize. Therefore, $FedF_{1–165}$ and two more truncates, $FedF_{1–160}$ and $FedF_{1–162}$, which are five and three amino-acid residues shorter (Fig. 1), respectively, were produced without a His tag. The construct for the shortest C-terminal truncate, $FedF_{1–160}$, did not express. $FedF_{1–162}$ and $FedF_{1–165}$ were purified as soluble proteins and set up for crystallization. However, no crystals could be obtained. In an attempt to make the FedF receptor-binding domain more amenable to crystallization (Buts *et*

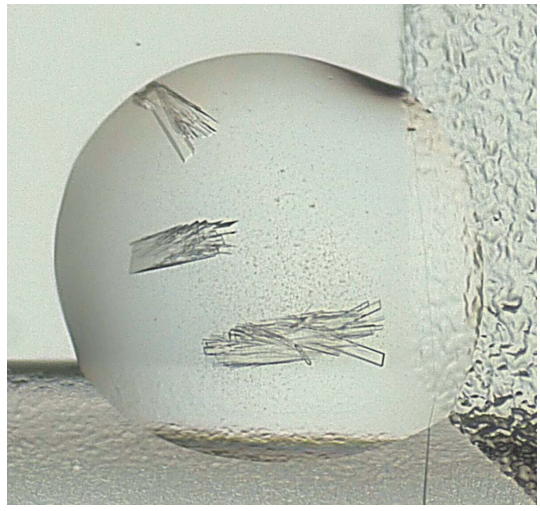

Figure 3
Crystals of $FedF_{15–165}$ grown at the EMBL high-throughput crystallization facility.

al., 2005), we purified $FedF_{v1–165}$ (Fig. 1) originating from a natural variant of the adhesin from the $F18^+$ *E. coli* strain 189P (Imberechts, CODA, Belgium). $FedF_{v1–165}$ also did not crystallize.

Remarkably, for all of the expressed soluble FedF truncates, the protein appeared as two close bands on SDS–PAGE, near the expected molecular weight of 18 kDa (Fig. 2). Moreover, both bands were also detected on Western blotting using the polyclonal rabbit antibody against FedF. The addition of reducing agents, such as 20 m*M* DTT, to the sample-loading buffer did not change this feature, indicating that this was not a consequence of incomplete disulfide reduction. N-terminal sequencing revealed two different N-termini, starting either at the expected residue or 14 residues later (Fig. 1). These results demonstrate that the FedF constructs were subject to a naturally occurring N-terminal cleavage. It was reasoned that the N-terminal heterogeneity could disturb the crystallization process. Two constructs encoding $FedF_{13–165}$ and $FedF_{15–165}$ were designed to match the shorter sequence of $FedF_{1–165}$ (Fig. 1). The signal sequence of the F4 fimbrial adhesin from *E. coli* was used because it is known to allow high levels of periplasmic FaeG. In $FedF_{13–165}$, the two residues preceding Asn15 were kept to resemble the cleavage site for the signal peptidase in FaeG. Nevertheless, the N-terminally truncated $FedF_{15–165}$ led to higher yields of soluble protein (Fig. 2). It was purified and set up for crystallization.

Crystals were obtained in one of the 500 conditions screened (Fig. 3). Although these crystals were smaller (300 × 40 × 40 µm) than those later reproduced in-house (1 × 0.2 × 0.1 mm), they diffracted considerably better (Table 1). It is most likely that the variable nonthermostatic conditions during setup are partly responsible for these differences, as the protein droplets tend to precipitate rapidly upon mixing at temperatures above 298 K in the laboratory. On the other hand, the temperature is well controlled in the crystallization robot and storage room.

Sugars that bind specifically to FedF may serve as a tool to solve its structure, as exemplified by the use of an Se derivative of GlcNAc (Buts, Loris *et al.*, 2003), or to obtain crystals in different space groups. The glycan array pointed out the recognition of *N*-acetyllactosamine units, Gal(β1-4)GlcNAc, that were either sulfated at position 3 and/or position 6 or fucosylated at position 2 of the galactose (Fig. 4). α1-Acid glycoprotein, which carries Gal(β1-4)-[Fuc(α1-3)]GlcNAc, was the best binding glycoconjugate. Other recognized carbohydrates were α1-2-fucosylated, namely Gal(α1-3)-[Fuc(α1-2)]Gal and the blood group H type II trisaccharide Fuc(α1-2)Gal(β1-4)GlcNAc (Fig. 4). Blood group H type II trisaccharide has previously been characterized as an F18 receptor (Snoeck *et al.*, 2004). (α1-2)-Fucosyltransferases have been implicated as being of importance for the presence of F18 receptors in piglets (Meijerink *et al.*, 1997, 2000). Trials to cocrystallize FedF in complex with several of these carbohydrates have so far remained unsuccessful.

Natural C-terminal truncates have been observed when overproducing recombinant tip adhesins, for example FimH and F17G. This possibly occurs as noncomplemented pilin domain of the adhesin becomes degraded. To date, N-terminal cleavage of tip adhesins has not been observed. It is therefore currently not understood what the mechanism and role of the cleavage of the 14-residue N-terminal truncation of $FedF_{1–165}$ is (Fig. 1). The N-terminal 14-residue sequence is very susceptible to proteolysis (http://www.expasy.org/tools/peptidecutter), whereas the amino-acid sequence just after the N-terminal truncation site (Asn15) is predicted not to be susceptible. Its sensitivity to proteolysis or hydrolysis could indicate that the structure of the N-terminal 14 residues behaves independently of the globular receptor-binding domain. Its length is reminiscent of the typical N-terminal extension that serves as a donor strand for the complementation of the incomplete Ig-fold of pilins. Moreover, its amino-acid sequence has an alternating hydrophobic–hydrophilic pattern and is conserved among variants (Fig. 1). Both those features are not present for the new N-terminus of the N-terminal truncate. If the 14 residues were a donor strand, this would have important implications. It would allow FedF to intercalate in the middle of F18 fimbriae by donating this N-terminal extension to a previous pilin in the pilus. In the absence of the 14-residue N-terminal sequence, FedF would be destined to reside only at the tip of F18 fimbriae. Solving the FedF crystal structure could shed light on this mechanism.

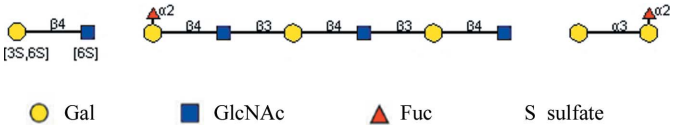

Figure 4
Glycoconjugates recognized by $FedF_{1–165}$ on a glycan array by the Consortium for Functional Glycomics.

We thank Liu Qiang from the Research Center of Centre Hospitalier de l'Université de Montreal, Canada for his help during the initiation of this project. We wish to thank Richard A. Alvarez, Director of Core H, for performing the glycan-array analysis, conducted by the Protein-Glycan Interaction Core H of the Consortium for Functional Glycomics funded by NIGMS grant GM62116. We are grateful to Dr Manfred Weiss, EMBL beamline scientist at X12 at the DESY synchrotron, Hamburg. JB is a postdoctoral fellow of the Fonds voor Wetenschappelijk Onderzoek–Vlaanderen, which also provided financial support (FWO-G.0513.04) and the DNA-sequencing equipment (FWO-AL215).

References

Bertschinger, H. U., Bachmann, M., Mettler, C., Pospischil, A., Schraner, E. M., Stamm, M., Sydler, T. & Wild, P. (1990). *Vet. Microbiol.* **25**, 267–281.
Blixt, O. *et al.* (2004). *Proc. Natl Acad. Sci. USA*, **101**, 17033–17038.
Bouckaert, J., Berglund, J., Schembri, M., De Genst, E., Cools, L., Wuhrer, M., Hung, C. S., Pinkner, J., Slättegård, R., Zavialov, A., Choudhury, D., Langermann, S., Hultgren, S., Wyns, L., Klemm, P., Oscarson, S., Knight, S. & De Greve, H. (2005). *Mol. Microbiol.* **55**, 441–455.
Buts, L., Bouckaert, J., De Genst, E., Loris, R., Oscarson, S., Lahmann, M., Messens, J., Brosens, E., Wyns, L. & De Greve, H. (2003). *Mol. Microbiol.* **49**, 705–715.
Buts, L., Loris, R., De Genst, E., Oscarson, S., Lahmann, M., Messens, J., Brosens, E., Wyns, L., De Greve, H. & Bouckaert, J. (2003). *Acta Cryst.* D**59**, 1012–1015.
Buts, L., Wellens, A., Van Molle, I., Wyns, L., Loris, R., Lahmann, M., Oscarson, S., De Greve, H. & Bouckaert, J. (2005). *Acta Cryst.* D**>61**, 1149–1159.
Choudhury, D., Thompson, A., Stojanoff, V., Langermann, S., Pinkner, J., Hultgren, S. J. & Knight, D. S. (1999). *Science*, **285**, 1061–1065.
Coligan, J. E., Dunn, B. M., Ploegh, H. L., Speicher, D. W. & Wingfield, P. T. (2002). Editors. *Current Protocols in Protein Science.* New York: Wiley.
Collaborative Computational Project, Number 4. (1994). *Acta Cryst.* D**50**, 760–763.
Dodson, K. W., Pinkner, J. S., Rose, T., Magnusson, G., Hultgren, S. J. & Waksman, G. (2001). *Cell*, **105**, 733–743.
Gyles, C., Johnson, R., Gao, A. L., Ziebell, K., Pierard, D., Aleksic, S. & Boerlin, P. (1998). *Appl. Environ. Microbiol.* **64**, 4134–4141.
Hahn, E., Wild, P., Schraner, E. M., Bertschinger, H. U., Häner, M., Müller, S. A. & Aebi, U. (2000). *J. Struct. Biol.* **132**, 241–250.
Imberechts, H., De Greve, H., Schlicker, C., Bouchet, H., Pohl, P., Charlier, G., Bertschinger, H., Wild, P., Vandekerckhove, J., Van Damme, J., Van Montagu, M. & Lintermans, P. (1992). *Infect. Immun.* **61**, 1963–1971.
Imberechts, H., Wild, P., Charlier, G., De Greve, H., Lintermans, P. & Pohl, P. (1996). *Microb. Pathog.* **21**, 183–192.

Jędrzejczak, R., Dauter, Z., Dauter, M., Piatek, R., Zalewska, B., Mroz, M., Bury, K., Nowicki, B. & Kur, J. (2006). *Acta Cryst.* D**62**, 157–164.
Kapitany, R. A., Forsyth, G. W., Scoot, A., Mckenzie, S. F. & Worthington, R. W. (1979). *Infect. Immun.* **26**, 173–177.
Korotkova, N., Le Trong, I., Samudrala, R., Korotkov, K., Van Loy, C. P., Bui, A. L., Moseley, S. L. & Stenkamp, R. E. (2006). *J. Biol. Chem.* **281**, 22367–22377.
Meijerink, E., Fries, R., Vogeli, P., Masabanda, J., Wigger, G., Stricker, C., Neuenschwander, S., Bertschinger, H. U. & Stranzinger, G. (1997). *Mamm. Genome*, **8**, 736–741.
Meijerink, E., Neuenschwander, S., Fries, R., Dinter, A., Bertschinger, H. U., Stranzinger, G. & Vogeli, P. (2000). *Immunogenetics*, **52**, 129–136.
Miroux, B. & Walker, J. E. (1996). *J. Mol. Biol.* **260**, 289–298.
Newman, J., Egan, D., Walter, T. S., Meged, R., Berry, I., Ben Jelloul, M., Sussman, J. L., Stuart, D. I. & Perrakis, A. (2005). *Acta Cryst.* D**61**, 1426–1431.
Otwinowski, Z. & Minor, W. (1997). *Methods Enzymol.* **276**, 307–326.
Pettigrew, D., Anderson, K. L., Billington, J., Cota, E., Simpson, P., Urvil, P., Rabuzin, F., Roversi, P., Nowicki, B., du Merle, L., Le Bouguenec, C., Matthews, S. & Lea, S. M. (2004). *J. Biol. Chem.* **279**, 46851–46857.
Rost, B. & Liu, J. (2003). *Nucleic Acids Res.* **31**, 3300–3304.
Sauer, F. G., Fütterer, K., Pinkner, J. S., Dodson, K. W., Hultgren, J. S. & Waksman, G. (1999). *Science*, **285**, 1058–1061.
Smeds, A., Hemmann, K., Jakava-Viljanen, M., Pelkonen, S., Imberechts, H. & Palva, A. (2001). *Infect. Immun.* **69**, 7941–7945.
Snoeck, V., Verdonck, F., Cox, E. & Goddeeris, B. M. (2004). *Vet. Microbiol.* **100**, 241–246.